Progress in the Self-Similar Turbulent Flame premixed combustion model

V. Moreau

CRS4, Environment and Imaging Science, Polaris Ed.1, I-09010 Pula (CA), Italy

Abstract

This paper is devoted to premixed combustion modeling in turbulent flow. First, we briefly remind the main features of the Self-Similar Turbulent Flame model that was more extensively developed in a former paper. Then, we carefully describe some improvements of the model. The determination of the turbulent flame velocity is based on the observed self-similarity of the turbulent flame and uses the local flame brush width as a fundamental parameter, which must be retrieved. With respect to the former version, we now derive more rigorously how the density variation has to be taken into account in the width retrieving function. We reformulate the diffusion term as a classical flux divergence term. We enforce the compatibility of the model for the limit of weak turbulence. We include a contracting effect of the source term, thus allowing to give a stationary mono-dimensional asymptotic solution with a finite width. We also include in a preliminary form, a stretch factor, which proves to be useful for controlling the flame behavior close to the flame holder and near the walls. The model implementation in the Star-CD CFD code is then tested on three different flame configurations. Finally, we shortly discuss the model improvements and the simulation results.

Key words: CFD, turbulent combustion, self-similarity, combustion modeling, premixed combustion

1 Introduction

It is now widely recognized that in many applications turbulent premixed combustion takes place in very thin corrugated flamelet sheets occupying an extremely small volume fraction of the flow domain [27,30]. As a consequence,

a natural asymptotic is the fast chemistry case in which the combustion region is approximated by a 2-dimensional manifold characterized only by a local propagation velocity. This framework leads to the individuation of two separated fluids, the fresh and the burned mixture, with their proper physical properties, temperature and velocity field, interacting through their common interface. The region occupied by each fluid is an unknown variable of the problem and it is practical to define it as a support function which is formally identical to the regress variable for the fresh mixture and to the progress variable for the burned mixture. At this point, a bifurcation occurs for the modeling.

One can choose to write separated averaged equations for each fluid and model their interaction. This is the Eulerian Reacting Two-phase flow approach [26]. This approach requires the use of an additional vector field (the second phase velocity) and the use of an additional scalar field (its mass fraction) and has a very strong potential. But (even non reacting) two-phase flows are still difficult to handle in standard commercial CFD codes. In particular, it is very difficult and maybe impossible for the basic user to stabilize flows in which some region must have zero as first phase volume fraction value.

Alternatively, one can recombine the two velocity fields to retrieve the usual unified global averaged velocity field, and recombine the progress and regress variable equations to get both the averaged density and progress variable equations (in the adiabatic incompressible case). In this way, some information is lost on the velocity field, but we have only one unclosed new averaged scalar equation for the progress variable. This approach, usually expressed in terms of probability density functions, has been introduced with the BML model [4] and is widely used in a number of models.

Following the analysis of [15,17], many of these models can be classified under three categories, depending on the progress variable source term closure:

- Algebraic models: the source term is essentially expressed by the ratio between some function of the mean progress variable and a characteristic time usually closely related to the turbulent time. In this category, we can find the model by Mason and Spalding [22], Magnussen and Hjertager [21], Bray and Moss [4], Bray [5,6], Zhao et al. [33], Bailly et al. [1] and Schmidt et al.[29].
- Flame Surface Density models also called Coherent Flame Models (CFM): the source term is proportional to the flame surface density Σ for which a balance equation is derived and closed. We have the model by Borghi [2], Candel et al. [7], Cant et al. [8], Cheng and Diringer [9], Boudier et al. [3], Duclos et al. [12], Choi and Hun [10] and Prasad and Gore [28].
- Gradient models: the source term $\bar{S} = \rho_u U_t |\nabla \tilde{c}|$ is proportional to the gradient of the mean progress variable. The models differ according to the

algebraic expression used for the burning velocity U_t. The first model of this kind is due to Zimont [34], which was followed and improved by Zimont and Lipatnikov [36,37] and Karpov et al. [13]. The burning velocity may also have been put explicitly dependent on time, like in Weller [32] and Lipatnikov and Chomiak [18,19].

Here, we are interested in the local burning velocity and consumption rate. Considering an hypothetical mono-dimensional transient flame in a frozen turbulent field, it is straightforward to see that:

- Using algebraic models, the burning velocity scales with the width;
- using gradient models, the burning velocity is independent of the width, except at the cost of an explicit time dependence;
- using Flame Surface Density models, the eventual relationship between velocity and width is not a priori obvious.

Therefore, if the dependence between local burning velocity and brush width exists but is not proportional, as demonstrated in [16], there is no simple model, without explicit time dependence, capable of taking clearly this property into account. The explicit time dependence for the source term is not really satisfying because it introduces some arbitrariness in the setting of the simulations, specially when considering complex stationary burning devices.

In a former paper [23], we have shown that is is possible to derive a simple model, the Self-Similar Turbulent Flame (SSTF) model, in which the relation between local burning velocity and brush width is evident but non trivial. In fact, the model is developed in a framework allowing any arbitrary a priori relationship between local burning velocity and brush width.

This paper is dedicated to a proper extension, taking into account additional features, of the SSTF model to multi-dimensional cases, its integration for CFD analysis and its validation, in the framework of premixed turbulent combustion.

For the mathematical description and derivation of the model, we use the same formalism adopted for the Turbulent Flame Closure (TFC) model [35] and the same structure of the mean progress variable equation $\tilde{c}$. The model construction is therefore reduced to the finding of an appropriate propagation velocity and a suitable diffusion-like term. Lipatnikov and Chomiak [15], from an extensive analysis of experimental data, have clearly highlighted that the flame brush has a strong self-similarity property as a function of the mean progress variable. The model proposed is based on this property. In fact, we invert the classical approach in which the self-similarity is checked a posteriori to validate the model. The main peculiarity of the SSTF model is the demonstration that the flame brush width can be effectively used as a fundamental parameter of the problem. Nevertheless, the former version of the model had

two major drawbacks. First, the effect of the density variation due to the temperature was taken into account in a completely empirical manner. Secondly, the velocity-based diffusion term was not by force of integral zero, which is a rather large drawback for a diffusion term. In the following, we introduce changes in the original model removing these two defects. Then, we add to the model additional features to extend its domain of validity. We introduce a contracting effect of the source term, enforcing the model compatibility with an asymptotically stationary mono-dimensional flame brush behavior with finite width. We also modify the source term to have a consistent behavior in the limit of weak turbulence and introduce a stretch factor which helps to control some flash-back phenomena (being it of numerical, modeling or physical nature) near the flame holder and close to the walls.

This modeling has been implemented in the Star-CD commercial CFD software through user routine programming and tested on three turbulent flame case studies.

2 Basis of the model

We shortly present here the basis at the origin of the SSTF model.

In premixed turbulent combustion, the turbulent flame brush exhibits strong self-similarity features [15]. It is now known that the flame is locally made of a highly corrugated flamelet sheet. In our study, we will suppose that the flame brush characteristics depend on the unstrained laminar flamelet parameters, on the turbulence parameters and eventually on time. We will use the subscript "l" for the laminar flamelet parameters and the subscript "t" for the turbulent brush parameters. For turbulence, the self-similarity parameter, according to Kolmogorov theory, is the energy dissipation ϵ. Laminar flamelets give small scale parameters and should not influence the flame brush self-similarity dimensionality. Moreover, we hope (and will suppose) that the laminar flamelet behavior will influence the flame brush characteristics only through a unique combination of fundamental parameters. Therefore, $\epsilon_t = \dfrac{U_t^3}{\delta_t}$, where U_t and δ_t are the flame brush velocity and width, is a good a priori choice. It is associated with the laminar flamelet parameter $\epsilon_l = \frac{S_l^3}{\delta_l} = \frac{S_l^4}{\chi}$ where S_l is the laminar flame speed, δ_l, its width and χ the gas diffusion. If ϵ_t is a self-similar parameter, then one of its simplest functional dependence on turbulence and laminar flamelet parameters is the following:

$$\epsilon_t = \epsilon^a \cdot \epsilon_l^{1-a}. \tag{1}$$

There is no explicit time dependence in the former expression because the self-

4

similarity property is time invariant. We expect the exponent a to be close to $\frac{1}{2}$ for various reasons given elsewhere [23], so from now on, we consider $a = \frac{1}{2}$.

Looking at the experimental results throughout literature, the flame brush appears to have a very clearly defined front. Its width is therefore better described by the distance δ_t between the boundary rather than by the mean dispersion. Clearly, thanks to the self similarity property, the two approaches give proportional results. So, we will address the brush width evolution having in mind the evolution of its forward and backward fronts. By analogy with classical turbulent diffusion propagation with front, we will consider that the enlargement speed is proportional to the turbulent pulsation. Since the width seems to be convected by the combined effect of the main flow and of the brush velocity, we arrive to the following symbolic representation:

$$\partial_t \delta_t + (u + U_t \cdot n) \cdot \nabla \delta_t = u', \tag{2}$$

where u' is the turbulent velocity pulsation and $U_t \cdot n$ the brush velocity.

In synthesis, our model is:

$$\epsilon_t = \epsilon^{0.5} \cdot \epsilon_l^{0.5}, \tag{3}$$
$$\partial_t \delta_t + (u + U_t \cdot n) \cdot \nabla \delta_t = u'. \tag{4}$$

We note that, in the case of anchored flames, the modulus of the advection velocity $u + U_t \cdot n$ decreases when the brush velocity U_t increases. Therefore, for a given distance from the flame holder, the brush has more time to increase. Finally, the model predicts an increase of the brush width when the flame brush velocity increases.

To implement this model in a CFD code, one must be able to evaluate locally δ_t. This is done using the self-similarity of the flame brush and choosing a reasonable shape. The local value of δ_t can thus be retrieved from the local value of $\tilde{c}$ and $|\nabla \tilde{c}|$. In effect, stating the self-similarity of the flame means $c = f(x/\delta)$ and by differentiation $\delta = \dfrac{f'(x/\delta)}{\partial_x c}$. This last expression is then generalized to multidimensional cases. The function f is chosen a priori. As the brush width is determined by the progress variable, we do not use equation (4) which in any case is un-practical to use as it is. Instead, the behavior described by this equation can be implemented in the mean progress variable equation by the inclusion of a diffusion velocity U_{diff} whose value depends on $\tilde{c}$ and which is compatible with the shape chosen. To be compatible with equation (4), we have to take $U_{diff} = f^{-1}(\tilde{c})u'$. The second order classical diffusion term of the $\tilde{c}$-equation is then replaced by $\overline{\rho} U_{diff} |\nabla \tilde{c}|$.

5

This methodology allows in principle to generate a diffusion region with a finite front velocity. And this velocity can be made dependent on the diffusion layer width.

Two constants A and B of order one are introduced in the CFD model to fit the experimental results. Finally, we have:

$$U_t = A\delta_t^{\frac{1}{3}}\epsilon^{\frac{1}{6}} \cdot \epsilon_l^{\frac{1}{6}}, \tag{5}$$

$$\text{``}[\nabla \cdot D_t \nabla \tilde{c}]'' = B\overline{\rho}U_{diff}|\nabla\tilde{c}|. \tag{6}$$

Hence, the implemented mean progress variable equation is:

$$\partial_t \overline{\rho}\tilde{c} + \nabla \cdot \overline{\rho}\tilde{u}\tilde{c} = B\overline{\rho}U_{diff}|\nabla\tilde{c}| + \rho_u U_t|\nabla\tilde{c}|. \tag{7}$$

From a practical point of view, we have initially used the following function family to retrieve the brush width:

$$\delta = [\frac{\sqrt{\rho_u\rho_b}}{\overline{\rho}}]^a \frac{[\tilde{c}(1-\tilde{c})]^b}{|\nabla\tilde{c}|} \tag{8}$$

with a and b between 0.5 and 1.

This modeling has been implemented in the Star-CD commercial CFD software through user routine programming and numerical results have been presented in [23].

Nevertheless, the RHS term in equation (6) is not satisfactory because it is not a pure diffusion term, not being by force of null integral. Moreover, the arbitrariness of the"δ" retrieving function is really excessive, mainly with regards to the density dependency.

3 Improvement of the model

3.1 Basics

The original unclosed progress variable equation reads:

$$\partial_t \overline{\rho c} + \nabla \cdot \overline{\rho}\tilde{u}\tilde{c} = \overline{\dot{S}} - \nabla \cdot \overline{\rho u''c''}. \tag{9}$$

Considering that $\rho_b \bar{c} = \bar{\rho}\tilde{c}$, where ρ_b is the (constant) density of the burned mixture, and defining S by $\rho_b S = \dot{\bar{S}} - \nabla \cdot \overline{\rho u" c"}$, equation (9) can be rewritten as:

$$\partial_t \bar{c} + \nabla \cdot (\tilde{u}\bar{c}) = S. \tag{10}$$

Taking into account that $\tilde{c}$ is function of $\bar{\rho}$, one can combine the mass equation and equation (9) to eliminate the time derivative term. One gets:

$$\nabla \cdot \tilde{u} = (1 - \frac{\rho_b}{\rho_u})S. \tag{11}$$

In order to address the density consistency problem, we now turn to the classical mono-dimensional case for which equation (11) can be integrated, giving:

$$\tilde{u} = u_0 + (1 - \frac{\rho_b}{\rho_u}) \int\limits_{-\infty}^{x} S. \tag{12}$$

We search a self-similar solution for which S has the functional form:

$$S = u_0 \partial_x F(\bar{c}, \delta) \tag{13}$$

where δ is a non better defined length depending only on time and having the vocation to become the self-similarity parameter.

Inserting equation (13) in equation (10), after some algebra, results in:

$$\partial_t \bar{c} + u_0 \partial_x (\bar{c} - \frac{\bar{\rho}}{\rho_u} F(\bar{c}, \delta)) = 0. \tag{14}$$

We need to separate the functional dependencies in $\bar{c}$ and δ, as follows:

$$\bar{c} - \frac{\bar{\rho}}{\rho_u} F(\bar{c}, \delta)) = H(\delta)G(\bar{c}). \tag{15}$$

This can be done taking:

$$F(\bar{c}, \delta)) = \frac{\rho_u}{\bar{\rho}} [\bar{c} - \frac{u_1}{u_0} H(\delta)G(\bar{c})]. \tag{16}$$

Noting g the derivative of G ($g = G'$), we have:

$$\partial_t \bar{c} + u_1 H(\delta) g(\bar{c}) \partial_x \bar{c} = 0. \tag{17}$$

This last equation has a self-similar solution whose profile is the inverse of the function g and whose time evolution is controlled by $u_1 H(\delta)$.

Turning back to the original source term, with some additional algebra, we obtain for the mono-dimensional case:

$$\overline{S} - \nabla \cdot \overline{\rho u'' \widetilde{c''}} = \rho_u u_0 \partial_x \tilde{c} - u_1 H(\delta) \partial_x [\frac{\rho_u \rho_b}{\bar{\rho}} G(\bar{c})]. \tag{18}$$

As usual, we must stress the fact that there is no a priori one to one correspondence between the two LHS and the two RHS terms. Nevertheless, in the following, we will report the first RHS term as the "source" term Σ and the second one as the "diffusion" term D.

3.1.1 Choice of Σ and D

A reasonable extension of the source term to the multidimensional case is:

$$\Sigma = \rho_u U_t |\nabla \tilde{c}| \tag{19}$$
$$= -\rho_u U_t n \cdot \nabla \tilde{c} \tag{20}$$

where U_t is now the turbulent burning velocity and n is the normal vector defined by $n = -\dfrac{\nabla \tilde{c}}{|\nabla \tilde{c}|}$.

The function G in equation 18 is defined up to a constant. If we add a constant to G, as $\dfrac{1}{\rho}$ is proportional to $\tilde{c}$, this constant part can be associated to the first RHS term in equation 18. Doing this, we are just stating that U_t can be dependent on δ and that we can take $G(0) = 0$ without loss of generality.

In the former version of the SSTF model, the diffusion term was velocity based and was written as a classical convective transport term. Here, we rewrite the mono-dimensional diffusion term in a gradient form easy to generalize in a divergence form, which is more classical and natural for a diffusion effect. We have:

$$D = -u_1 H(\delta) \partial_x [\frac{\rho_u \rho_b}{\bar{\rho}} G(\bar{c})] \tag{21}$$

$$= \partial_x [u_1 H(\delta) \frac{\rho_u \rho_b}{\bar{\rho}} G(\bar{c}) n]. \tag{22}$$

Here, $n = -1$ is the normal to the front for a fresh mixture at x negative: $n = -\dfrac{\partial_x \tilde{c}}{|\partial_x \tilde{c}|}$ or $n = -\dfrac{\partial_x \bar{c}}{|\partial_x \bar{c}|}$. In the turbulence context, the velocity u_1

should be strongly linked to the turbulent velocity pulsation u' and we have the following natural extension of equation (22) to the multi-dimensional case:

$$D = \nabla \cdot [u' H(\delta) \frac{\rho_u \rho_b}{\bar{\rho}} G(\bar{c}) n]. \tag{23}$$

An interesting particular case is when $H(\delta) = \frac{L}{\delta}$ where L is proportional to the integral length scale. Recalling that $\delta = \frac{1}{g'(\bar{c})|\nabla \bar{c}|}$, we have:

$$
\begin{aligned}
D &= \nabla \cdot [u' L g'(\bar{c}) G(\bar{c}) \frac{\rho_u \rho_b}{\bar{\rho}} \nabla \bar{c}] \\
&= \nabla \cdot [u' L g'(\bar{c}) G(\bar{c}) \bar{\rho} \nabla \tilde{c}] \\
&= \nabla \cdot [D_t g'(\bar{c}) G(\bar{c}) \bar{\rho} \nabla \tilde{c}]
\end{aligned} \tag{24}
$$

where D_t is proportional to the turbulent diffusion.

This means that when the profile is based on the error function (primitive of a Gaussian), then $g'G$ is a constant independent from c. As $g'(0) = +\infty$, this situation is realized only if $G(0) = 0$. For other reasonable profiles, to have $D_t g'(\bar{c}) G(\bar{c})$ bounded, it is necessary (but not sufficient) that $G(0) = 0$. Consistently with the possible dependency of U_t on δ, hereinafter we consider that $G(0) = 0$ (and therefore, we have $G \leq 0$).

Equation 24 shows that our diffusion term is both i) a generalization of the classical diffusion term because it is not restricted to the error function profile and to only one temporal behavior, and ii) a restriction of the classical diffusion term because it can be applied only to normalized front profiles.

One can remark that, while the progress variable equation is stated in terms of the Favre variable, that is a mean weighted by density, the profile is naturally set in term of the Reynolds variable, that is a mean weighted by the volume. This is more consistent with the feeling that diffusion is fundamentally an exchange of volumes with different concentrations. It is also clear that for self-similar profiles of finite length, if the $\tilde{c}-$profile is symmetrical, then the $\bar{c}-$profile is not, and reciprocally. We will focus our attention to profiles which are symmetrical in terms of the Reynolds variable.

In light of these considerations, we give an updated general representation form for the diffusion term rewriting equation (23) as:

$$D = \nabla \cdot [D_t \frac{H(\delta) G(\bar{c})}{L |\nabla \bar{c}|} \bar{\rho} \nabla \tilde{c}] \tag{25}$$

and if we introduce the turbulent flame Prandtl number

$x \in$	$[-\frac{\pi}{2}, \frac{\pi}{2}]$	$[-1, 1]$	$]-\infty, +\infty[$	$]-\infty, +\infty[$
f	$\frac{sin(x)+1}{2}$	$\frac{1+x\sqrt{2-x^2}}{2}$	$\frac{e^x}{1+e^x}$	$\frac{1+erf(x)}{2}$
g	$\arcsin(2c-1)$	$c^{0.5} - (1-c)^{0.5}$	$\ln(\frac{c}{1-c})$	$-$
g'	$\dfrac{1}{\sqrt{c(1-c)}}$	$\dfrac{c^{-0.5} + (1-c)^{-0.5}}{2}$	$\dfrac{1}{c(1-c)}$	$-$
G	$-\sqrt{c(1-c)}$ $+\frac{(2c-1)\arcsin(2c-1)-\frac{\pi}{2}}{2}$	$\frac{2}{3}[c^{1.5} + (1-c)^{1.5} - 1]$	$c\ln c$ $+(1-c)\ln(1-c)$	$-$
$g'G$	1 $+\frac{(2c-1)\arcsin(2c-1)-\frac{\pi}{2}}{2\sqrt{c(1-c)}}$	$\frac{-1}{3}\sqrt{c(1-c)}$ $\times[2 - \frac{1}{(1+c^{0.5})(1+(1-c)^{0.5})}]$	$\frac{c\ln c+(1-c)\ln(1-c)}{c(1-c)}$	$-C_1$
$g'G(0)$	0	0	$-\infty$	$-C_1$
$g'G(0.5)$	$1 - \frac{\pi}{2}$	$-\frac{1+\sqrt{2}}{6}$	$-4\ln 2$	$-C_1$

Table 1

Tentative profiles of function f with their inverse g, the primitive G and the derivative g' of the inverse. The exact value of C_1 is yet unknown but is strictly positive (about 1) and finite.

$$\sigma = -\frac{L|\nabla \bar{c}|}{H(\delta)G(\bar{c})} = \frac{-L}{\delta H(\delta)g'(\bar{c})G(\bar{c})} \tag{26}$$

we revert to the classical form

$$D = -\nabla \cdot [\frac{D_t}{\sigma}\bar{\rho}\nabla\tilde{c}]. \tag{27}$$

3.1.2 Choice of the profile

At this point, we are faced with the problem of choosing a reasonable and practical profile. By saying reasonable, we mean quite regular (with at least one continuous derivative), monotonous, with only one inflexion point having a non zero finite slope. By saying practical, we mean explicit, with explicit inverse (g) and explicit primitive of the inverse (G).

In table 1, we can see that if we want to have a non-standard self-similar evolution of the profile, we just do not know how to do it easily for an error function based profile. The exponential profile would have been an optimum candidate because it has the great property that the Reynolds and Favre profiles are identical, just shifted one from the other. Unfortunately, it gives for the standard diffusion time behavior a diffusion coefficient that goes to infinity for $c = 0$ and $c = 1$. The sinusoidal and square root based profiles are both relatively acceptable. The square root based profile has the slight advantage that the product $-g'G$ can be put in a form that avoids indeterminate ratio which

always need to be carefully treated numerically. A minor drawback of these two last profiles is that they belong only to the class C^1 (that is, continuous with continuous first derivative), because their curvature is discontinuous at $c = 0$ and $c = 1$. Looking forward to improve this regularity, we can see that if g' behaves like $c^{1/n-1}$ close to $c = 0$, then the profile regularity is of class C^{n-1}. This observation naturally leads to consider the following profiles:

$$g(c) = N(n)[c^{1/n} - (1 - c)^{1/n}] \tag{28}$$

where the parameter n is greater than 2 and $N(n)$ is a normalization factor such that $-g'G(1/2) = 1$ and determined as

$$N(n) = \frac{\sqrt{n+1}}{2\sqrt{0.5^{1/n} - 0.5^{2/n}}}. \tag{29}$$

The case $n = 2$ is given in table 1. For n greater than 2, there is no practical explicit profile. But, as the profile f is never explicitly used, it does not give rise to practical implementation problems.

Looking at the function $-g'G$ for different values of n, we can see that between $n = 2$ and $n = 6$, it looks strongly like the function $[c(1 - c)]^{1/n}$, seemingly tending to a flat profile for larger n. Unfortunately, for $n = 7$ and greater, the maximum is no more in $c = 0.5$ and the shape is no more convenient. This restrict the field of interesting values for n to integers between 2 and 6; or, if we want a continuous curvature, between 3 and 6. We can find help to make this choice looking at the ratio between the length given by the effective width of the profile and the length based on the profile derivative in $x = 0$ or $c = 0.5$ for different n,

$$\delta_{bound} = g(1) - g(0) = \sqrt{n+1}[0.5^{1/n} - 0.5^{2/n}] \tag{30}$$

$$\delta_{slope} = g'(0.5) = 2^{1-1/n}\frac{\sqrt{n+1}}{n}[0.5^{1/n} - 0.5^{2/n}] \tag{31}$$

then

$$\delta_{slope} = \frac{2^{1-1/n}}{n}\delta_{bound}. \tag{32}$$

These ratios are given in table 2.

In the following, we will consider $n = 3$, which is the minimum integer giving a continuous curvature and giving a length ratio of about 0.5, which seems a

11

n	1	2	3	4	5	6
$\dfrac{\delta_{slope}}{\delta_{bound}}$	1	0.71	0.53	0.42	0.35	0.30

Table 2
Ratio of the length based on the maximum slope to the length based on distance between the boundaries for different values of the parameter n

reasonable value. Higher values of n lead to stiffer functions that may be more difficult to handle numerically while not giving relevant improvements.

3.2 Additional features

The model improvements discussed up to now deal with the issues that were individuated in the former version of the model. The additional features presented hereafter are of a less fundamental nature but help widening the range of application of the model. As these features are not always essential, they are included in such a way that they can easily be switched on or off. In this manner, their numerical implementation can be managed with a simple parameter file. Furthermore, they illustrate how easily some flame behavior can be installed in the equation once we have access to the flame brush width as a local variable.

3.2.1 Short time/width behavior

Looking back to equation 25, we still have to make decision concerning the shape of the function $H(\delta)$. According to the standard turbulent diffusion theory, a sharp front should enlarge at constant speed, while a smeared front has an enlargement rate proportional to the inverse of its width. Taking the turbulent length scale as the reference scale, this means:

$$H(\delta) \sim 1 \text{ for } \delta \ll L \tag{33}$$

$$H(\delta) \sim \frac{L}{\delta} \text{ for } \delta > L. \tag{34}$$

This behavior can be reproduced just by setting:

$$H(\delta) = \frac{1}{\sqrt{1 + (\frac{\delta}{L})^2}}. \tag{35}$$

Numerically, it is conveniently implemented using a "switch" parameter, say "Ini" (for Initial), with value one (on) or zero (off) and writing:

$$H(\delta) = \frac{1}{\sqrt{1 + Ini \cdot (\frac{\delta}{L})^2}}. \tag{36}$$

3.2.2 Contracting effect of the source term

In the specific case of reactive flows, the turbulent flame brush can be constrained to have a maximum width due to a slight contracting effect of the real source term. For example, one can consider that the integral contracting effect of the real source term is proportional both to S_l and to δ, or alternatively, proportional to S_l and independent from δ, remembering that this effect may not be perceived for a brush width of order L. As the integral turbulent diffusion effect scales like D_t/δ, the combined diffusion term should go to zero when $S_l(\delta/L)^a$, with $a = 1$ or $a = 0$, is of order D_t/δ, and this regardless of the modeling of the purely convective part of the source. Modeling separately the contracting effect of the real source term, for consistency, we should rewrite equation 23 and following with S_l instead of u' and with $H(\delta) = (\delta/L)^a$:

$$Cont = \nabla \cdot [S_l \frac{\delta^a G(\bar{c})}{L^a |\nabla \bar{c}|} \bar{\rho} \nabla \tilde{c}] \tag{37}$$

or

$$Cont = \nabla \cdot [C_f \bar{\rho} \nabla \tilde{c}] \tag{38}$$

$$C_f = \frac{S_l \delta^{1+a} g'(\bar{c}) G(\bar{c})}{L^a} \tag{39}$$

defining in this way the "flame contraction coefficient" C_f.

In the end, the turbulent flame diffusion coefficient D_f is:

$$D_f = \frac{D_t}{\sigma} - C_f. \tag{40}$$

The turbulent diffusion D_t is proportional to the turbulent viscosity, both being related through the Schmidt number Sch whose value for reacting scalars is usually taken equal to $Sch = 0.7$. Since our treatment (even without contracting term) essentially reduces the turbulent diffusion value, but is not intended to modify its mean value, we take $Sch = 0.6$ to approximately compensate this effect.

Solving $D_f = 0$ in equation 40, we get the asymptotic brush width δ_∞ and the asymptotic flame brush velocity $U_{f\infty}$. Considering $H(\delta) = L/\delta$ for the

diffusion term (giving the expected normal diffusion behavior for large enough diffusing fronts), the result is:

$$\delta_\infty = L(u'/S_l)^{1/(1+a)} \tag{41}$$

$$U_{f\infty} = u'(S_l/u')^{(3a+1)/6(1+a)}(L/\delta_l)^{1/6}. \tag{42}$$

This last formula can be expressed in terms of the traditional non dimensional numbers, the turbulent Reynolds number $Re_t = \frac{u'L}{S_l\delta_l}$, the Damköhler number $Da = \frac{L/u'}{\delta_l/S_l}$ and the Karlovitz number $Ka = (\frac{u'}{S_l})^2 Re^{-1/2}$.

$$U_{f\infty} = u' Da^{(2a+1)/6(1+a)} Re_t^{-a/6(1+a)} = u' Da^{1/6} Ka^{-a/3(1+a)}. \tag{43}$$

In order to keep a small contribution for the contracting term even for brush widths somewhat greater than the turbulent length scale, we will consider $a = 0$ in the following, then:

$$C_f = S_l \delta g'(\bar{c}) G(\bar{c}) \tag{44}$$

$$\delta_\infty = L(u'/S_l) \tag{45}$$

$$U_{f\infty} = u'(S_l/u')^{1/6}(L/\delta_l)^{1/6} = u' Da^{1/6}. \tag{46}$$

It should be noted that these last considerations have generally no practical effect on real flame modeling because there are apparently no known existing highly turbulent flame wide enough to critically sense the contracting effect. By the way, for a pure theoretical point of view, we provide the model with a stationary mono-dimensional solution. Moreover, we also get a sound limit both for δ and U_f, for example when the profile is highly disturbed near the walls.

Another way to decide the asymptotic length is to state that the asymptotic sped is independent from the laminar flame properties, as in [38]. This directly leads to the following formula:

$$\delta_\infty = L(\epsilon/\epsilon_l)^{1/2} = (L \cdot \delta_l)^{1/2}(u'/S_l)^{3/2} \tag{47}$$

$$U_{f\infty} = u'. \tag{48}$$

This formula seems sound only when ϵ is greater than ϵ_l otherwise the asymptotic brush width would be smaller than L. It should be noted that the terminal velocities in equations 46 and 48 are very similar while the brush width may be quite different, showing that is it hazardous to try to deduce the terminal brush width from equilibrium considerations on the terminal flame velocity.

More generally, the problem is that also U_f is likely to be involved in the mechanism creating the contraction. A better attention paid to the contracting effect is likely to lead to a different expression in a future model improvement.

If, by chance, in an hypothetical case, the contracting effect is a relevant feature, and due to changes in the turbulence parameters, the brush is larger than the asymptotic limit, then the diffusion term becomes negative. In this kind of cases, it may be wiser to incorporate the contracting effect into the source term, using equation (22) with $u_1 = -S_l$ to get:

$$Cont = S_l H(\delta) \rho_u \rho_b \partial_{\tilde{c}} \frac{G(\bar{c})}{\bar{\rho}} |\nabla \tilde{c}|. \tag{49}$$

In alternative, the contracting term can be split in two parts, one canceling the diffusion term setting the diffusion coefficient (close) to zero, and the residual part added to the source term.

This approach, while not applied in this paper, shall be preferred for an eventual extension of the model in the framework of Large Eddy Simulation (LES). Moreover, requiring that the contracting effect scales naturally with the LES filter size should help better define the contracting term.

3.2.3   Low Reynolds Asymptotic behavior

The SSTF model is thought primarily for highly turbulent flows whose turbulent pulsation is quite larger than the laminar flame velocity. And therefore, the model has not a correct behavior when turbulence becomes arbitrarily small. A simple remedy to this is provided by adding the Laminar flame velocity to the turbulent part. To get eventually a smooth transition from one regime to the other, or to not overestimate the flame brush velocity when the laminar and the turbulent velocities are about the same, we combine both velocities through some exponent α to define the Low Reynolds turbulent Flame velocity in the following form:

$$U_{fLR} = (U_f^\alpha + S_l^\alpha)^{1/\alpha}. \tag{50}$$

with α a priori close to the interval $[1, 2]$. For simplicity and homogeneity in the notation, we choose to take $\alpha = 2$.

For numerical implementation, also here we use a switch parameter, say Lrab (from the subsection title), with value zero or one and writing:

$$U_{fLR} = (U_f^2 + Lrab \cdot S_l^2)^{1/2}. \tag{51}$$

3.2.4 Wall treatment by quenching

For the mean progress variable, the boundary condition used in presence of a solid wall is the no flux condition, that is a zero gradient normal to the wall. This condition is not satisfying because it is contradictory with the profile shape. The result is that the brush width is highly overestimated close to the walls and this may lead to the appearance, development and propagation of a spurious flame along these walls. A simple way to eliminate this spurious flame is to give an upper limit to the flame width. There are two relatively natural limits which can be taken into consideration. The first one comes from the eventual theoretical estimation of the mono-dimensional stationary asymptotic width. The second limit, much more prosaic, is to state that the brush width cannot be larger than the available space. Anyway, whatever reasonable limiting criteria was expected to remove this problem without other effects on the simulation. In practice, this procedure is not always sufficient to prevent the flame from rising back along the wall. When the flow has time to develop, the turbulent dissipation tends to be very high along the wall, several orders higher than the dissipation in the mean flow. Therefore, the flame burning speed is also quite high there, due to its functional dependency. Looking for a sound criteria to limit this velocity, we found out that we neglected any possible stretch induced local extinction effect. In [39], the problem has been treated introducing a critical dissipation ϵ_{crit} proportional to the laminar flame dissipation ϵ_l with a quite large proportionality coefficient. When the turbulent dissipation increases up to order ϵ_{crit} there is an increasing probability to have the flame locally quenched, and therefore the flame velocity must be correspondingly damped. Following the same argument, we will replace the turbulent dissipation by an effective (or damped) turbulent dissipation ϵ_{eff} in the definition of the flame brush velocity. We set:

$$\epsilon_{eff} = \frac{\epsilon}{(1 + \frac{\epsilon^2}{\epsilon_{crit}^2})^{3/2}} \tag{52}$$

$$\epsilon_{crit} = \quad B^2 \cdot 15\epsilon_l \tag{53}$$

with B about 2 from first preliminary simulations. The exponent $3/2$ at the denominator is chosen so that the perturbation acts at power $1/2$ in the source term. In case one uses the Low Reynolds variant, it is wiser to damp also the laminar part.

The quite high coefficient (corresponding also to $B = 2$ in the cited paper) can be justified by the extremely high intermittency of the real dissipation. While for the applications shown hereafter, this features is used to get rid of wall boundary problems, a deeper attention in the future could give the possibility to effectively contribute to the simulation of some flash-back phenomena.

3.2.5   Source overshot

From the numerical point of view, the source term in the progress variable equation is not a transport term and is not constrained by some maximum principle. The result is that close to the burned flame brush boundary, mainly when the brush is very sharp, the progress variable overcomes unity at the end of each algorithm iteration. While the value is reset to unity at the beginning of each iteration, the profile is modified and reaches unity with a not so small slope, leading to an apparent local brush width which is extremely sharp. As the source term depends on the width, it is locally reduced by this mechanism, and in some way the overshoot is self-controlled. This may be however a concern for the diffusion which goes to zero if one uses the diffusion control for small brush width. One can limit the smallest value of the apparent width, for example, to the laminar flame width or to the computational cell width. Some tests (not shown here) indicate that there is no substantial change induced by the way the progress variable is limited, except for the automatic scale displayed when visualizing the sharpness field (the inverse width field). This problematic must be kept in mind, understanding that when the flame brush width is very small, then the flame speed and diffusion is rather altered by numerics. This can be a challenging issue for a future adaptation of the model for LES, where the flame width is expected to remain everywhere quite small.

4   Numerical implementation and results

Hereafter, we show some simulations performed using the updated SSTF model. The modeling has been implemented in the Star-CD (version 4.02) commercial CFD software through user routine programming. All numerical results presented here are the result of Star-CD simulations. The numerical test cases are the same as the one presented for the preliminary version of the SSTF model. The first series of simulation is based on a V-shaped flame and is compared with visual experimental data given in [11]. The second test case is based on a Volvo experimental facility. The flame is maintained by a central triangular flame holder. The simulation is based on the one presented earlier and based also on input data given in [24]. The third test case is the Moreau burner as reported in [40] and [20].

4.1   System of equations

Unless otherwise noted, the simulations have been performed with the following parameters:

17

- $g(c) = N(3)[c^{1/3} - (1-c)^{1/3}]$ (that is $n = 3$ in equation 28)
- The width is defined by $\delta = \frac{2}{g'(\bar{c})|\nabla\bar{c}|}$ and is limited by the asymptotic length
- $H(\delta) = \frac{L}{\delta}$ that is $\frac{1}{\sigma} = g'(\bar{c})G(\bar{c})$ in equation 27
- $a = 0$ in equation 37, that is $C_f = S_l\delta g'(\bar{c})G(\bar{c})$ and the contracting term is effective
- $\alpha = 2$ in equation 50, that is $U_{fLR} = (U_f^2 + S_l^2)^{1/2}$.
- $B = 2$ in equation 53 and ϵ_{eff} is effectively used.
- $A = 0.6$, in equation 6, that is $U_f = 0.6\delta^{1/3}\epsilon_l^{1/3}\epsilon^{1/3}$
- In the end, the source term is: $\Sigma = \rho_u\left(\frac{S_l^2 + 0.6^2\delta^{2/3}\epsilon_l^{2/3}\epsilon^{2/3}}{1 + (\frac{\epsilon}{60\epsilon_l})^2}\right)^{\frac{1}{2}}|\nabla\tilde{c}|$.

The flows simulated are considered adiabatic (no thermal diffusive flux) and incompressible (no pressure dependence of the density). The temperature T_u and density ρ_u of the fresh (unburned) mixture are both set to a case dependant constant. The burned temperature T_b is also a constant, either given or retrieved from thermo-chemical consideration. The burned density is normally approximately obtained from the perfect gas law.

The fundamental set of variables consists of the Reynolds averaged density $\bar{\rho}$, the Favre averaged velocity $\tilde{u}$ and the Favre averaged progress variable $\tilde{c}$. The set of solved equations is based on the averaged Navier-Stokes equations for density and momentum [31]. For the flow simulated, they reduce to:

$$\partial_t\bar{\rho} + \nabla \cdot (\bar{\rho}\tilde{u}) = 0 \tag{54}$$

$$\partial_t(\bar{\rho}\tilde{u}) + \nabla \cdot (\bar{\rho}\tilde{u}\tilde{u}) + \nabla\bar{P} - \nabla \cdot (\mu_{eff}\Pi\tilde{u}) = \bar{\rho}g \tag{55}$$

Here, $\bar{P}$ is the mean pressure, the effective viscosity $\mu_{eff} = \mu_t + mu_l$ is the sum of the laminar and turbulent viscosity, g is the gravity acceleration and the differential operator Π is defined by $\Pi v = \nabla v + \nabla^T v - \frac{2}{3}(\nabla \cdot v)I$, where I is the identity matrix.

The turbulent viscosity is obtained from a $\kappa - \epsilon$ turbulence model [14] requiring to solve two additional transport equations, one for the turbulence energy κ and one from its dissipation ϵ.

The mean density and the mean temperature are algebraic functions of the progress variable and set through user subroutines:

$$\bar{\rho} = \left(\frac{\tilde{c}}{\rho_b} + \frac{1-\tilde{c}}{\rho_u}\right)^{-1}, \tag{56}$$

$$\tilde{T} = \tilde{c}T_b + (1-\tilde{c})T_u. \tag{57}$$

The progress variable is obtained by solving a passive scalar transport equation:

18

$$\partial_t \bar{\rho}\tilde{c} + \nabla \cdot (\bar{\rho}\tilde{u}\tilde{c}) - \nabla \cdot (\frac{\mu_{eff}}{\sigma}\nabla\tilde{c}) = \Sigma, \tag{58}$$

with σ (according to equation 26) and S defined through user subroutines.

4.2 Numerical implementation

The user subroutines needed to implement this modeling are directly accessible from the standard release of the StarCD software. The only non-standard feature is the necessity to compute the gradient of the progress variable. A subroutine giving access to this possibility has been readily provided by CD-Adapco upon simple request.

All the simulations have been run using wherever possible the default setting of the software. They have been performed in steady state using the SIMPLE solution algorithm [25]. The turbulence model chosen is the $\kappa - \epsilon$ High Reynolds Number one [14] together with the standard Wall Function. The spatial differencing scheme is the Monotone Advection Reconstruction Scheme (MARS) for the momentum, turbulence and progress variable. It is Central Differencing (CD) for the density.

The meshes used are simple, two-dimensional and block structured. They are illustrated in figure 1. Cell numbers are 37,040 for the V-shaped flame (only half domain is effectively simulated), 21,504 for the Volvo burner and 12,500 for the Moreau burner. The geometries are over simplified. For example, the round cylinder of the V-shaped flame is numerically "approximated" by a squared one. Simulation time to get a stationary solution was quite short, no more than a few minutes and a few hundred of iterations running on a standard PC.

We used the Neumann (no flux) boundary condition for the progress variable on all the wall boundaries. So, the flame was nowhere artificially anchored to the flame holder as happens when a unit Dirichlet boundary condition is used. When needed, combustion was started by forcing the progress variable to unit in a small region behind the flame holder once a cold flow has been established. The forcing had to last only for one iteration.

The mesh density was chosen in order both to have fast results and to capture the features under examination giving reasonably smooth colormap results. No investigation on the dependence or independence of the results on the mesh density has been performed. This investigation, which could be the object of future works is much less trivial than it seems. In fact, the combustion modeling is combined with the turbulence modeling. And the turbulence modeling is mesh dependent because of the wall functions for which the non dimensional

distance from the wall Y+ must stay in a defined range. As we have already observed the onset of flash back phenomena with a tendency of the flame to rise back along the walls (Moreau Burner), getting mesh independence would require the perfect control of this flash back phenomena, which is far beyond the object of this paper.
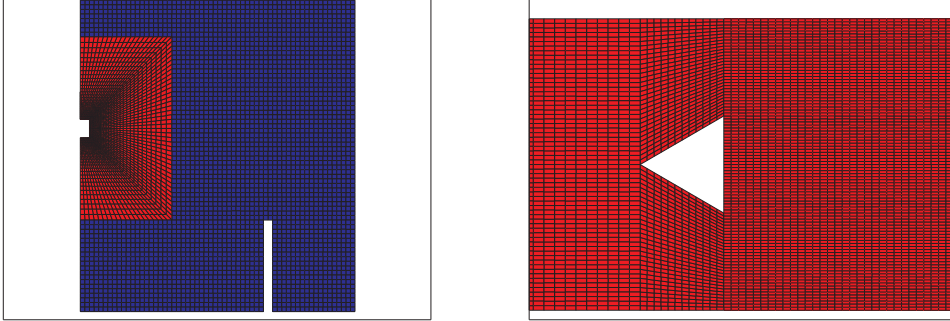

Fig. 1. Details of the mesh used, on the left for the V-shaped flame and on the right for the Volvo burner.

4.3   Turbulent premixed V-shaped flame

The SSTF model is compared with experimental data on an experimental test case performed by F. Dinkelacker and S. Holzler and described in [11]. This setup is neither really axial-symmetrical nor Cartesian 2-dimensional. Differences in the simulations resulted to be quite marginal in former simulations and we present only Cartesian 2-D simulations. Note that the constants A and α of the SSTF model have been tuned precisely on this model. The model gives very good results compared with the experimental results. It gives the same global shape and the same tendency.

The mixture inlet is 2.5m/s in vertical at ambient room temperature. The laminar speeds used in the simulations are respectively 0.19, 0.10 and 0.04 m/s and are not expected to be very accurate. The diffusion coefficient is taken equal to the air cinematic viscosity (Hypothesis of unit Lewis number), that is $1.57E - 5m^2/s$. There is also a vertical co-flow at 0.5 m/s to avoid strong lateral boundary effects.

The experimental results are showed in figure 2. It is not totally clear what is the meaning of the figure, in terms of the calculated variable. Nevertheless, we will suppose that the apparent flame position is a good indicator of the progress variable. When dealing with visual observation, the weight averaging in the Favre-averaged progress is probably not taken into account. The Reynolds averaged progress variable seems therefore more suitable for comparison, as is also considered in [11]. In order to evaluate the flame position, both variables are essentially shifted between each other for a not so small fraction of the local

brush width. In figure 3 and 4, we present the simulated profile respectively of the Reynolds and Favre progress variable. In figure 5, we show the effect of the critical stress limitation which is almost non effective when B=2 (RHS), but moves the flame anchoring from under the flame holder to the lateral part of the flame holder when B=1 (LHS).
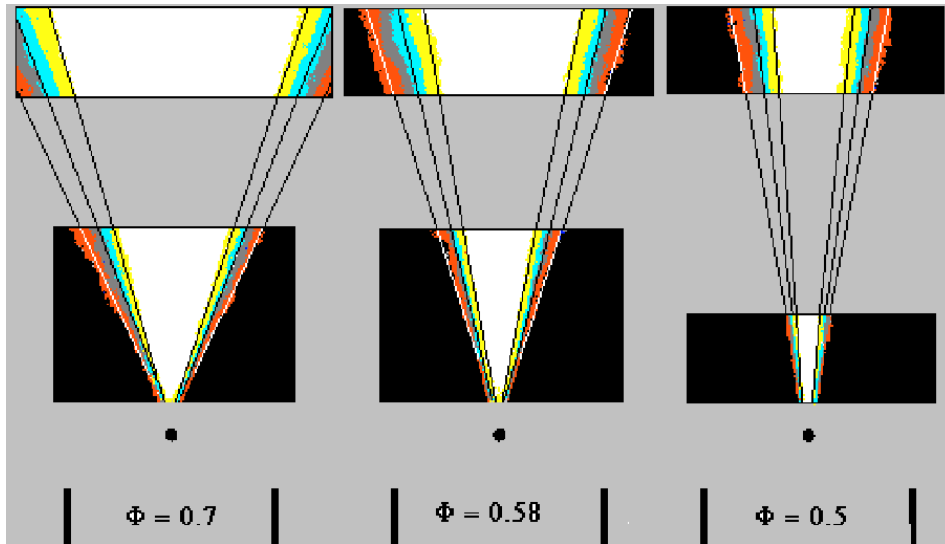

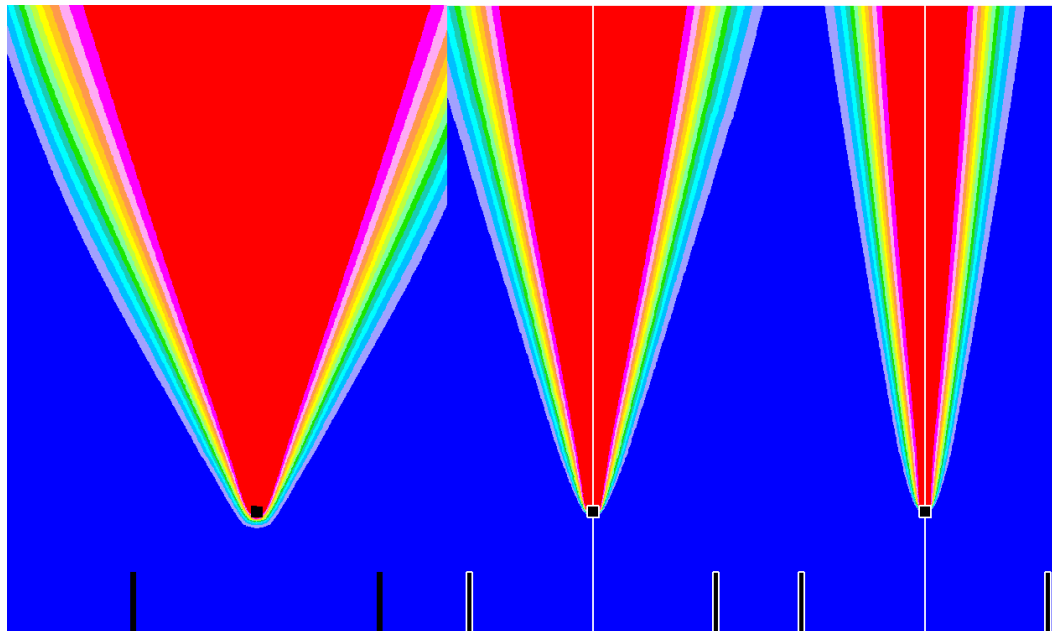Fig. 2. Experimental results: Soika, 1996; Dinkelacker, Holzler, Leipertz, 1999

Fig. 3. V-shaped flame. From left to right, the mean Reynolds averaged progress variable $\bar{c}$ for $\phi = 0.7$, $\phi = 0.58$ and $\phi = 0.5$. Parameters are: A=0.6 and B=2.
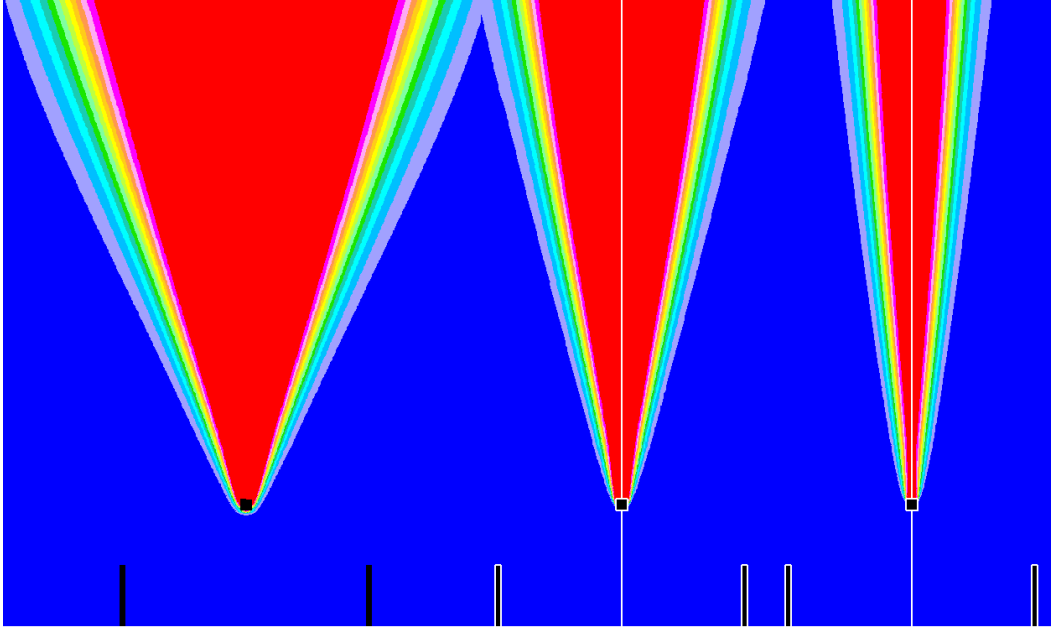
Fig. 4. V-shaped flame. From left to right, the mean Favre averaged progress variable $\tilde{c}$ for $\phi = 0.7$, $\phi = 0.58$ and $\phi = 0.5$. Parameters are: A=0.6 and B=2.
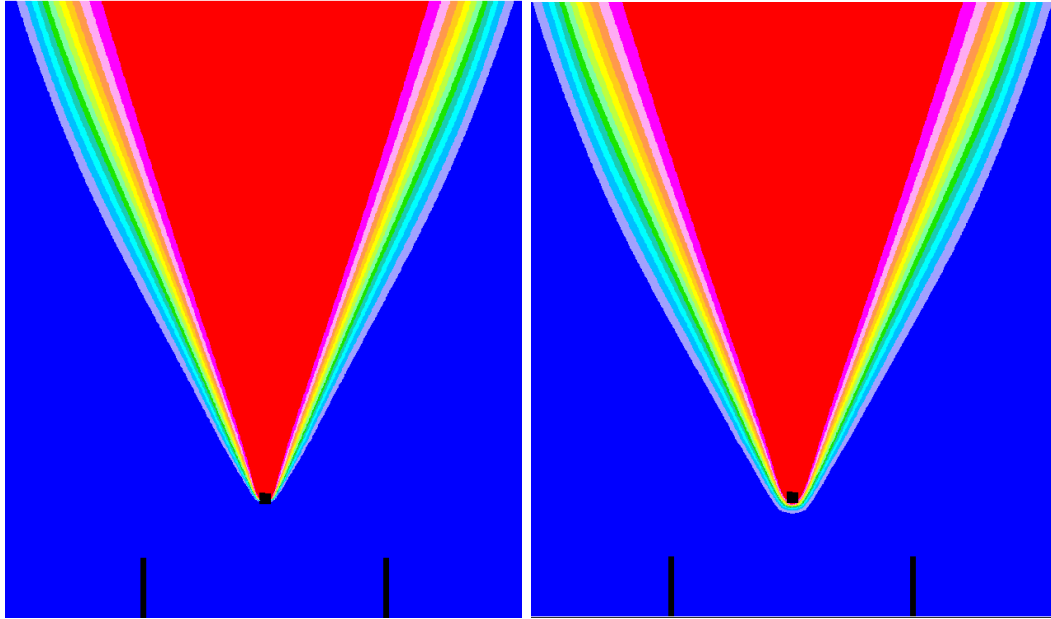

Fig. 5. V-shaped flame. Mean Reynolds averaged progress variable $\bar{c}$ for $\phi = 0.7$ and A=0.6. On the LHS B=1 and on the RHS B=2.

4.4 Volvo burner

This test case has been inspired from [24]. Parameters of the problem are: inlet velocity $18m/s$, turbulent intensity 3%, and length scale $8mm$. Molecular diffusivity $2.E - 5m^2/s$, $A = 0.6$ laminar flame speed $0.743m/s$. Inlet temperature 600 K and burned temperature 1850 K. The flame holder is $4cm$

high in a rectangular channel 12 cm high and 24 cm wide. The problem can be reasonably represented in two dimension. The simulated domain extends up to 60 cm from the flame holder. In figure 6, we show the Favre averaged progress variable in the given configuration (top) and with the parameter B changed from 2 to 4 (bottom). The difference can be seen near the walls close to the outlet. For the standard configuration, there is almost no flash-back effect while the flash-back effect can be clearly seen when the stretch effect control has been reduced.
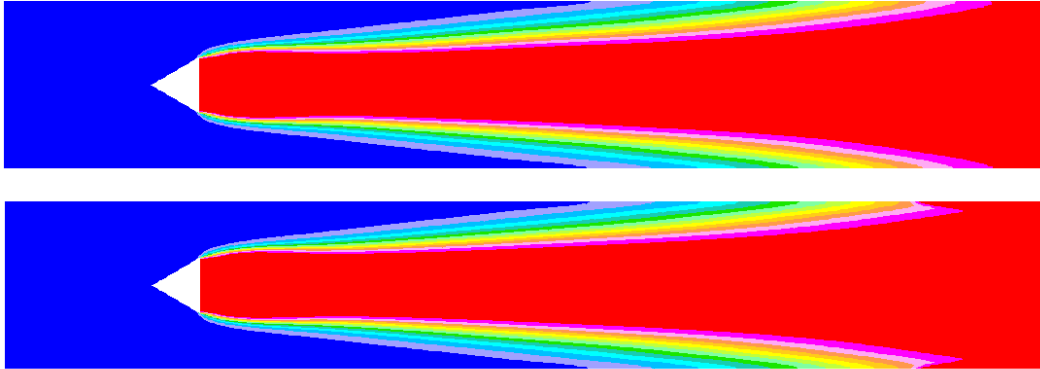

Fig. 6. Favre Progress Variable for the Volvo burner Simulation. Upper, standard configuration, lower, parameter B controlling the stretch effect has been moved from 2 to 4.

The former parameters resulted, after control, unfit. The results should be interpreted only as a technical demonstration of feasibility. In[24], the inlet velocity is in fact about $34.1m/s$ and after control the diffusion coefficient is taken as $\chi = 5.27E^{-5}$. But the simulation resulted unstable with large oscillations and it was not possible to get a converged stationary solution. This is illustrated in figure 7. Note that the presence of large Von Karman like vortices was noticed during the experiment as reported in [24]. So, it is normal not to have any stationary solution in the RANS framework. A stationary solution, obtained by simulating only one half of the domain would be therefore highly misleading.
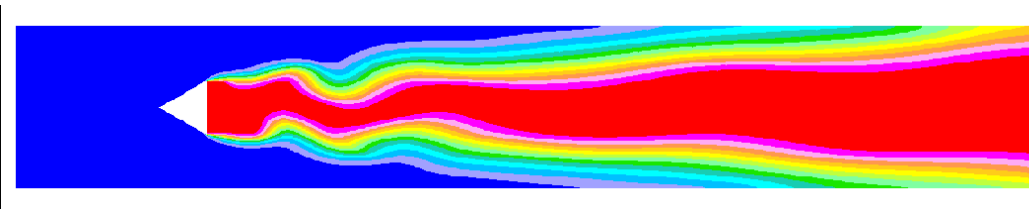

Fig. 7. Favre Progress Variable for the Volvo burner Simulation. Inlet velocity 34.1 m/s, turbulence intensity 10%, $A = 0.6$. Transient, non converged simulation.

phase	T(K)	$\rho, kg.m^{-3}$	u (m/s)	u' (m/s)	$\kappa(m^2.s^{-2})$	$\epsilon(m^2.s^{-3})$	ϕ
burned	2240	0.1538	120	23	793	$2.8E6$	0.87
unburned	600	0.562	60	8	100	3.7E4	0.87

Table 3

Moreau burner test case. Inlet flow conditions for burned and unburned mixture

4.5 Moreau burner

The simulation of the Moreau burner is taken from [40] and [20]. The inlet conditions are given in table 3. We used a laminar flame velocity of 1.15 m/s and a molecular diffusivity of $5.27E - 5m^2.s^{-1}$. The computational domain is 100 mm high for 1300 mm long, with 12500 cells.

In figure (8), we show the progress variable in the computational domain. In the top image, $B = 1$ while in the bottom one, $B = 2$. The difference is very small and is concentrated close to the inlets junction. For $B = 1$, the combustion is slightly more delayed.
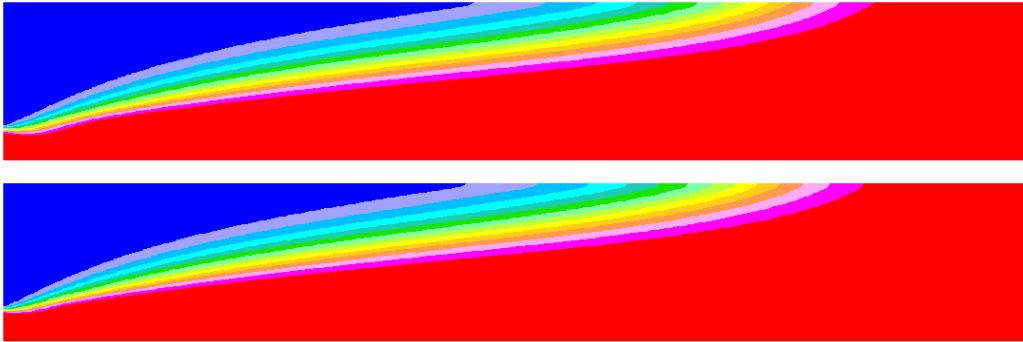

Fig. 8. Moreau burner. TFC and standard $\kappa - \epsilon$ model. Progress variable. The flows enter from the left. Computational model is 100 mm high and 1300 mm long. Top picture, $B = 1$. Bottom picture, $B = 2$.

5 Discussion

In [23], we have proposed a turbulent flame brush model based on the Kolmogorov theory of turbulence and the self-similarity. By using a priori the concept of self-similarity of the flame brush width, we can obtain locally a correct estimation of the brush width. Considering the reverse of the usual Taylor hypothesis on the equivalence of time and space dependence, we have

in fact given access to the time dependence for modeling. As a side product, the self-similarity together with the access to the width allows to construct a diffusion term with a non classical behavior. First, the diffusion front can travel at finite velocity. Second, the diffusion strength can be made dependent on the width. This can be useful for example to model the initial part of the brush for which the standard diffusion theory gives a time dependence. These features can be introduced modifying the diffusion coefficient in the standard diffusion term. A drawback of the velocity based diffusion term was that, in the form proposed in [23], it was not neutral for the global consumption rate. Here, we have modified the form of the diffusion term, expressing it in the usual divergence form so as to ensure that it is a pure diffusion term.

Another problem linked with the former version of the SSTF model was the effective width retrieving function. This function can be analytically found for very simple configurations in which there is no density change, no shear and constant turbulent quantities. In this case, it depends on the expression used for the diffusion velocity term. Most problematic, was the density dependence that was implemented into the width retrieving function. This aspect is now largely clarified and the arbitrariness of the density dependency has been removed from the current model version.

The SSTF model has been derived mainly on the basis of the most simple assumption. Its basic assumption was that the chemistry affects the model through only one parameter: the "energy dissipation". This strong assumption had to be somewhat relaxed. In effect, in its original form, the SSTF model was not compatible with three asymptotic cases i) when the turbulent pulsation becomes the same order or smaller than the laminar flame velocity, ii) when the turbulence is so high than the flamelet structure completely disappears and iii) for the description of the academic stationary mono-dimensional behavior.

The first asymptotic case is simply treated by adding the laminar flame velocity to the burning velocity through their square values, summing in fact their "energetic strength". This introduces the laminar flame speed as a new chemical independent parameter, which is against the basic assumption of only one chemical parameter. For the time being, we have to accept this little "renouncement". The second asymptotic case is treated through the introduction of a damping multiplier of the source term, depending only on the turbulent and "laminar" energy dissipation. So, we are still consistent with the assumption of only one parameter. The damping factor proves to be very effective in controlling some flash-back phenomena in the Volvo-burner simulation, and the kind of attachment to the flame holder for the V-shaped flame. It deserves therefore much more attention and may be the object of future model development. The third asymptotic case is treated through the inclusion of a turbulent flame contracting (or anti-diffusive) effect. This effect is embedded in the diffusion term in such a way that the diffusion vanishes when the

asymptotic width is reached. Its implementation also helps to avoid absurd unbounded flame velocities near walls or some other potential pathological situations, in which a non trivial extrema or saddle-point (or "saddle-line in 3D) of the progress variable may appear. In the current implementation, the limiting width is based on an assumption which involves the appearance of the laminar flame speed as another "chemical" parameter, as for the first case. A greater care should be dedicated to this aspect and there are foreseeable changes in future model development.

There is still room for improvements in modeling into at least two directions:

- The damping of the diffusion when the brush width is very small is not yet tested. This has a direct effect on the local flame velocity because the flame brush erroneously enlarges too quickly in the vicinity of the flame holder or anchoring point. This aspect is of secondary importance for the evaluation of a priori stable flames (with no risk of blow-off). Nevertheless, it may become a critical point if we want to have some evaluation of the blow-off behavior when it is linked to the detachment of the flame from the flame holder.
- The contracting effect of the turbulent flame must be generalized to perform correctly even when it is greater than the turbulent diffusion. This is mainly a technical problem linked to the fact that the diffusion term in the CFD algorithm must absolutely have a non-negative diffusion coefficient. Having a both way controlling term, i. e., having a term able to effectively re-contract the brush width when suited seems to be an essential prerequisite to design a LES version of the model.

In [23], the fitting for the three cases considered lead to the parameter A ranging from 0.5 to 0.9. The rational and the improvements given to the model allow to perform again all the simulations with always the same constant $A = 0.6$.

6 Conclusion

We have included some improvements in a turbulent flame brush model based on self-similarity, simple chemistry coupling and Kolmogorov turbulent theory. The improved model has been implemented in the Star-CD commercial software and tested on three simulations where it gives very satisfying results. In this model, we consider that the brush width is a fundamental parameter which must be retrieved. The density variation is now consistently taken into account, both in the width retrieving function and in the dissipation term. Several modifications have been included to be consistent at least with

three asymptotic behaviors. The fitting constant A controlling the local brush speed is shown to be much less case dependent than in the former version of the model.

7 Acknowledments

References

[1] P. Bailly, M. Champion and D. Garreton, Counter Gradient diffusion in a confined turbulent premixed flame, *Phys. Fluids,* 9 (1997) 766.

[2] R. Borghi, Turbulent Premixed Combustion: Further discussions of the scales of fluctuations, *Combust. Flame* 8 (1990) 304.

[3] P. Boudier, S. Henriot, T. Poinsot and T. Baritaud, A model for turblent flame ignition and propagation in spark ignition engine. *Proc. Combust. Inst.* 24 (1992) 503 .

[4] K.N.C. Bray and J.B. Moss, A unified statistical model of the premixed turbulent flame, *Acta Astronautica* 4 (1977) 291

[5] K.N.C. Bray, Turbulent flows with premixed reactants, *Turbulent Reacting Flows*, Springer, Berlin, 1980, pp. 115-183

[6] K.N.C. Bray, Studies of the turbulent velocity, *Proc. R. Soc. London* A431 (1990) 315

[7] S. Candel, D. Veynante, F. Lacas, E. Maistret, N. Darabiha and T. Poinsot, Coherent flame model: Applications and recent extensions, *Advances in Combustion Modeling*, World Scientific, Singapore, 1990, pp.19-64.

[8] R.S. Cant, S.B. Pope and K.N.C. Bray, Modelling of flamelet surface-to-volume ratio in turbulent premixed combustion. *Proc. Combust. Inst.* 23 (1990) 809 .

[9] W.K. Cheng and J.A. Diringer, Numerical modelling of SI engine combustion with a flame sheet model. *SAE Paper 910268*, 1991

[10] C.R. Choi and K.Y. Hun, Development of a coherent flamelet model for spark-ignited turbulent premixed flame in a closed vessel. *Combust. Flame* 114 (1998) 336 .

[11] F. Dinkelacker and S. Holzer, Investigation of a Turbulent Flame Speed Closure Approach for Premixed Flame Calculation, *Combust. Sci. and Technol.* 158 (2000) 321-340

[12] J.M. Duclos, D. Veynante and T. Poinsot, A comparison of flamelet models for premixed turbulent combustion, *Combust. Flame* 95 (1993) 101.

[13] V.P. Karpov, A.N. Lipatnikova and V.L. Zimont, A test of an engineering model of premixed turbulent combustion. *Proc. Combust. Inst.* 26 (1996) 249.

[14] B.E. Launder and D.B. Spalding, The numerical computation of turbulent flows, *Comp. Meth. in Appl. Mech. and Eng.*,3 (1974),pp. 269-289

[15] A.N. Lipatnikov and J. Chomiak, Developing Premixed Turbulent Flames: Part 1. A Self-Similar Regime of Flame Propagation, *Combust. Sci. Technol.* 162 (2001) 85-112

[16] A.N. Lipatnikov and J. Chomiak, Turbulent flame sped and thickness: phenomenology, evaluation. and application in multi-dimensional simulations, *Prog. Energy Combust. Sci.* 28 (2002) 1-74.

[17] A.N. Lipatnikov and J. Chomiak, A study of the effects of pressure-driven transport on developing turbulent flame structure and propagation, *Combust. Theory Model.* 8 (2004) 211-225.

[18] A.N. Lipatnikov and J. Chomiak, A simple model of unsteady turbulent flame propagation. *J. Engines, SAE Transactions*, 106 (SAE paper 972993, 1997) 2441.

[19] A.N. Lipatnikov and J. Chomiak, Transient and geometrical effects in expanding turbulent flames. *Combust. Sci. Technol.* 154 (2000) 75.

[20] L. Maciocco and V.L. Zimont, Test of the TFS Combustion Model on High Velocity Premixed CH4-air Combustion in a channel, *20-th Annual Meeting of the Italian Section of the Combustion Institute*, 1997.

[21] B.F Magnussen and B.H. Hjertager, On mathematical modeling of turbulent combustion with special emphasis on soot formation and combustion, *Proc. Combust. Inst.* 16 (1976) 719

[22] H.B. Mason and D.B. Spalding, Prediction of reaction rates in turbulent premixed boundary layer flow, in: *Proceedings of the Combustion Institute European Symposium*, Academic Press, New York, 1973 pp. 601-606.

[23] V. Moreau, A Self-Similar Premixed Turblent Flame Model, *Appl. Math. Modell.* (2008), doi:10.1016/j.apm.2007.12.005

[24] P. Nilsson and X.S. Bai, Effects of flame stretch and wrinkling on CO formation in turbulent premixed combustion *Proc. Combust. Inst.* 29 (2002) 1873-1879

[25] S.V. Patankar and D.B. Spalding, A calculation procedure for heat, mass and momentum transfer in three-dimensional parabolic flows, *Int. J. Heat Mass Transfer*,15 (1972), pp. 1787-1806

[26] K. Pericleous and N.C. Markatos, A two-fluid approach to the modelling of three-dimensional turbulent flames, *Proc. Eurotherm, vol. 17, Springer Verlag, Cascais Portugal*, 1990.

[27] N. Peters, Turbulent Combustion. *Cambridge University Press*, 2000

[28] R.O.S. Prasad and J.P. Gore, An evaluation of flame surface density models for turbulent premixed jet flames. *Combust. Flame* 116 (1999) 1.

[29] H.P. Schmidt, P. HabisReuther and W. Leuckel, A model for calculating heat release in premixed turbulent flames *Combust. Flame*, 113,79 (1998).

[30] D. Veynante and L. Vervisch, Turbulent combustion modeling. *Prog. Energy Combust. Sci.* 28 (2002) 193-266.

[31] Z.W.A. Warsi, Conservation form of the Navier-Stokes equations in general nonsteady coordinates, *AIAA Journal, 19, pp.240-242*, 1981.

[32] H.G. Weller, The development of a new flame area combustion model using conditional averaging. *TF/9307, Mechanical Engineering Department, Imperial College*, 1993.

[33] X. Zhao, R.D. Matthiews and J.L. Ellzey, Numerical simulations of combustion in SI engines: Comparison of the Fractal Flame Model to the Coherent Flame Model, *Int. Symposium COMODIA98,JSME*, Tokyo, pp.157-162.

[34] V.L. Zimont To computations of turbulent combustion of partially premixed gases. *Chemical Physics of Combustion and Explosion Processes. Combustion of multi-phase and Gas System, OIKhF, Chernogolovka*, 1977, pp.77-80 (in Russian).

[35] V. Zimont, F. Biagioli and K. Syed, Modeling Turbulent Premixed Combustion in the Intermediate Steady Propagation Regime, *Int. J.:Prog. Comput. Fluid Dynam.* 1 (2001) 14-28.

[36] V.L. Zimont and A.N. Lipatnikov, To computations of the heat release rate in turbulent flames, *Dokl. Phys. Chem.* 1 (Russian original 1993, translated 1994) 332,592.

[37] V.L. Zimont and A.N. Lipatnikov, A numerical model of premixed turbulent combustion. *Chem. Phys. Reports* 14 (1995) 993.

[38] V.L. Zimont, Kolmogorov's Legacy and Turbulent Premixed Combustion Modeling *New Devel. in Combustion Research*, 2006, pp. 1-93, ISBN: 1-59454-826-9

[39] V.L. Zimont and F. Biagioli, Gradient , counter-gradient transport and their transition in turbulent premixed flames *Combust. Theory Model.* 6 (2002) 79-101.

[40] V.L. Zimont, M. Barbato and F. Murgia, On the Limits of Industrial Premixed Combustion Simulation Models, *Mediterranean Combustion Symposium,*the Combustion Institute 1999, June 20-25, pp. 372-383